Optical Pumping of Dye-Complexed and -Sensitized Porous Silicon Increasing Photoluminescence Emission Rates

J. L. Gole,* J. A. DeVincentis, and L. Seals

School of Physics, Georgia Institute of Technology, Atlanta, Georgia 30332-0430

Received: September 3, 1998; In Final Form: December 2, 1998

Distinctly structured nanoporous and combined hybrid macroporous−nanoporous porous silicon (PS) structures have been fabricated and treated with the dyes 3,3′-diethyloxadicarbocyanine iodide (DODCI) and Rhodamine 700, both of which have negligible absorption at the wavelengths of maximum absorption for porous silicon. After an extended period of aging in darkness (air) these dye-treated samples are pumped (PLE) at 337.1 nm (nitrogen laser) near the maximum in the PS absorption spectrum (far from the major absorption regions of the impregnating dye) and the subsequent photoluminescence from these treated samples is monitored and compared to that obtained for the untreated PS structures. The first time-dependent photoluminescence (PL) histograms obtained for these systems indicate that the resulting luminescence, initiated through the pumping of a modified PS surface, displays the manifestation of a significant interaction between the surface-bound fluorophors which characterize PS and the dye (DODCI). It is suggested that this interaction results in the creation of a distribution of PS−dye complexes which greatly enhance the nominal PL emission rate from the untreated PS surface. This enhancement not only facilitates the observation of luminescence from a formed photoluminescing PS "green" precursor state but also the mapping of its time-dependent oxidation to form the more commonly observed "orange-red" emitter. Both emitters are attributed to surface-bound silanone-based silicon oxyhydride fluorophors. The degree of PS−dye interaction, in addition to being dye dependent, is found to be PS-structure dependent. Thus the photoluminescent histograms obtained in this study also appear to provide evidence for the influence of PS morphology on the surface interaction.

Introduction

High-surface-area porous silicon (PS) structures formed in wafer scale through electrochemical (EC) etching display a visible photoluminescence (PL) 550−800 nm (∼2.25−1.5 eV)) upon excitation (PLE) with a variety of visible and ultraviolet light sources.[1−5] This room-temperature luminescence has attracted considerable attention, primarily because of its potential use in the development of silicon-based optoelectronics, displays, and sensors. However, the relatively long excited-state lifetime associated with this luminescence which appears to be of the order of tens to hundreds of microseconds[6] is problematic for some of these applications.

While the PS luminescence is thought to occur near the surface,[7,8] the source of the visible emission is controversial. The light-induced PL from PS has been associated with a variety of mechanisms, including emission from quantum-confined silicon crystallites,[7−13] surface-localized states,[7,8,14] surface-confined defects[15,16] or surface-confined molecular[17−20] or molecule-like[21−25] emitters. The efficiency and wavelength range of the emitted light can be affected by the physical and electronic structure of the surface,[3] the nature of the etching solution,[22,23,25] and the nature of the environment into which the etched sample is placed.[26−28]

The environment-dependent behavior of a PS surface suggests the possibility that several common fluorescent dyes whose radiative lifetimes are of the order of nanoseconds might be made to interact with the PS surface so as to considerably improve its observed luminescence rate. Here, we report a series of experiments designed to evaluate the interaction of select fluorescent dyes with PS samples of varying porosity and photovoltaic response.[29] We wish to obtain a strong physisorption or chemisorption of certain of these fluorescent dyes with the PS surface in order to gain control of and enhance the quantum yield and/or modify the lifetime of the fluorescent events associated with these PS structures.

The limited number of published reports[30−33] which have examined the interaction of dyes with PS exclusively involve nanoporous silicon generated from aqueous etchants. Two of these studies attempt to excite the dye and observe the effect of the PS matrix on the dye fluorescence.[30,31] Attempts to directly excite PS and observe energy transfer to the dye and the dye's resultant fluorescence or to excite a PS−dye complex and observe the emission from this complex have also been reported.[32,33] While the focus of these experiments is clearly energy transfer from the host PS surface, the broad absorption range of virtually all common laser dyes has limited the information that can be obtained from these studies. Therefore, the present study was designed to evaluate *energy transfer from PS* to a very limited group of impregnating dyes with negligible absorbance at wavelengths commensurate with the PS excitation spectrum. We find that the introduction of these laser dyes to the PS surface greatly enhances the characteristic features observed in a PL histogram as we monitor a modification of the time-dependent behavior of the photoluminescence. The changes induced are not only dye dependent but vary with the degree of exposure of the PS surface and the porosity of the surface.

* Author to whom correspondence should be addressed.

10.1021/jp983614n CCC: $18.00
Published on Web 01/26/1999

Experimental Section

Single-crystal (100) boron-doped silicon wafers with resistivities of the order 50−100 ohm-cm were obtained from Wafer World. The overall experimental configuration used to prepare aqueous samples of PS in a 25% HF in methanol etching solution (1 part concentrated HF: 3 parts methanol) and to monitor laser-induced photoluminescence from PS has been discussed elsewhere[23] and will only be briefly outlined. To prepare the aqueous samples, a 300 nm thin film of aluminum was sputtered onto the backside of the wafers. Ohmic contacts were made to the wafer by connecting a wire to the thin film of aluminum using conductive paint (Insulating Materials Inc., Ekote #3030). The wire and aluminum film were then covered with a layer of black wax (Apiezon W), leaving only the front surface of the silicon exposed to the etching solution. During the in situ etching process, both the silicon wafer wire and platinum electrode connections passed through a Teflon cap which was tightly fit to a cuvette in which the etching process was carried out. Etching currents ranged from 2 to 30 mA/cm^2 with the samples used in the present study etched at 8 mA/cm^2 for 10 min.

Hybrid nanoporous−macroporous PS samples were fabricated in an electrochemical cell constructed from high-density polyethylene. The working electrode was attached to the back of a p-type silicon wafer (100) and the counter electrode corresponded to a piece of platinum foil placed in solution. The cell was sealed to the front of the wafer, using a clamp, as a 1 cm^2 section of the wafer made contact with the solution. A magnetic stir-bar was used to prevent the buildup of hydrogen at the surface of the silicon. The electrochemical etching current was supplied by an EG and G Princeton Applied Research Potentiostat/Galvanostat (Model 273). The samples were etched in a solution of 1M H_2O, 1M HF, 0.1M tetrabutylammonium perchlorate (TBAP), all in acetonitrile, with a current density of 8mA/cm^2 for 75 min. Using this configuration, pores approximately 1 to 2 μm wide by 100 μm deep were formed, well-covered by regions of nanoporous silicon. To prepare these hybrid samples, an annealed aluminum contact was applied to the back of the silicon wafer prior to the etch.

Prepared aqueous and hybrid samples were removed from the etching solution, washed in reagent grade methanol (Fisher Optima 99.9%), and treated with 10^{-3} M (in doubly distilled H_2O) DODCI (3,3′-diethyloxadicarbocyanine iodide-Lambda Physik 99$^+$%) or Rhodamine 700 (Lambda Physik 99$^+$%). The porous silicon samples were dipped for several seconds or soaked for periods extending to 45 min.[33]

The hybrid and aqueous samples were both studied (ex situ) in air after their preparation. For the photoluminescence experiments described here, the output from a pulsed nitrogen laser at 337.1 nm was expanded and sent through a mask to the treated PS surface. The PS photoluminescence was dispersed, through a McPherson monochromator (which was scanned using a computer interfaced stepping motor), and impinged on a Hammamatsu 446 phototube. In order to perform time-dependent measurements with as small as a 5 ns delay after the laser pulse, a high-quality cutoff filter (Oriel Instruments dichroic #66237) is placed in front of the entrance slit to the monochromator. This filter, which transmits in the range 350−1200 nm at an average transmittance of 85%, blocks stray scattered light from the photoluminescence excitation nitrogen laser. The output from the phototube was sent to an SR400 (Stanford Research Series) photon counter where it was studied as a function of delay time after the laser pulse (at 0.5 μs intervals), each scan being taken with a 5 μs gate.

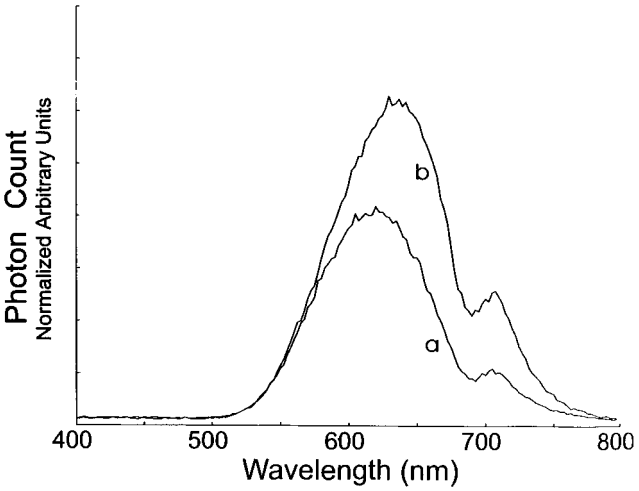

Figure 1. Comparison of time-gated 1.5−100 μs scans of the photoluminescent emission from porous silicon (PS) following excitation of (a) a nanoporous PS sample generated in an aqueous etch, and (b) a hybrid macroporous−nanoporous PS sample. Excitation is with a nitrogen laser at 337.1 nm. Uncorrected for system response which dips slightly at ∼690 nm.

The output from the photon counter was processed using an IBM PC-compatible counter. A typical scan, first from 400 to 800 nm in 2.5 nm steps with 40 laser shots per data point for the laser running with a repetition rate of 10 Hz, requires 25 min. This scan is immediately taken in reverse, furnishing a consistent internal check for any possible changes which might occur during the scan cycle. Spectral calibration could be accomplished with a mercury lamp or the individual laser excitation wavelengths, often in second order.

Results

Pore Structure and Photoluminescent Emission from Porous Silicon−Untreated Samples. Figures 1 and 2 display the time-dependent photoluminescent emission from aqueous and hybrid etched porous silicon samples. In Figure 1, we compare the photoluminescent emission observed over the period 1.5−100 μs after excitation (PLE) at 337.1 nm ($t = 0$). These normalized spectra represent the sum of all emission observed over the 98.5 μs time gate. These data suggest that the photoluminescence observed for the hybrid etched sample exceeds that for the aqueous etched sample and demonstrates a slight ∼10−15 nm red shift.

In Figure 2, parts a and b, we display a more detailed picture of the time-dependent photoluminescence as we present histograms for aqueous and hybrid etched samples which demonstrate the evolution of the photoluminescence giving rise to the overall appearance of the features in Figure 1. These spectra, taken with gate widths of 5 μs and delays after excitation (PLE) ranging from 0.5 to 9.5 μs, furnish emission histograms from which the comparative effect of dye treatment on the PS structures can be evaluated.

Porous silicon is known to display a "green" luminescence resulting from an intermediate precursor state formed in the earlier stages of its creation. This luminescence is especially evident in an aqueous etch solution.[22] The temporal decay and spectral profile of the "green" luminescence and its transformation to a final "orange-red" PL emission[22] during and following PS formation suggest the coupling of these luminescent emitters to the PS surface. In the histograms of Figure 2, at 0.5 μs, we observe the manifestation of the green and orange-red emission features in spectra which are virtually identical for the aqueous

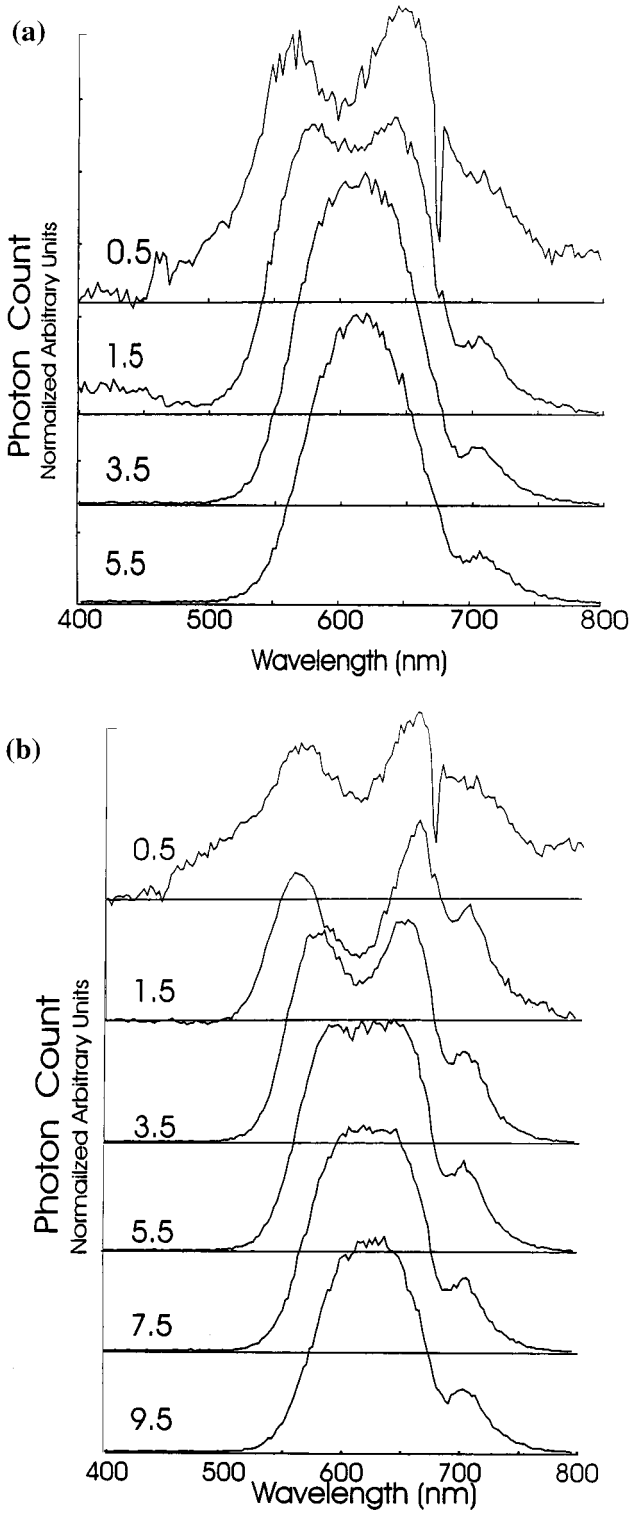

Figure 2. Photoluminescence histograms of (a) a nanoporous porous silicon (PS) sample for delay times after nitrogen (337.1 nm) laser pumping, of 0.5−5.5 μs each with a 5 μs gate, and (b) a hybrid macroporous−nanoporous PS sample for delay times, after nitrogen laser pumping of 0.5−9.5 μs each with a 5 μs gate. Uncorrected for system response. See text for discussion.

and hybrid etched samples. These histograms represent the first clear observation of the "green" luminescence feature in an air-aged sample and demonstrate the magnitude of its contribution to the overall spectrum.[29] With increasing delay time, (1) the "green" and "orange-red" emission features merge into each other as the source of the green emitter has undergone oxidative

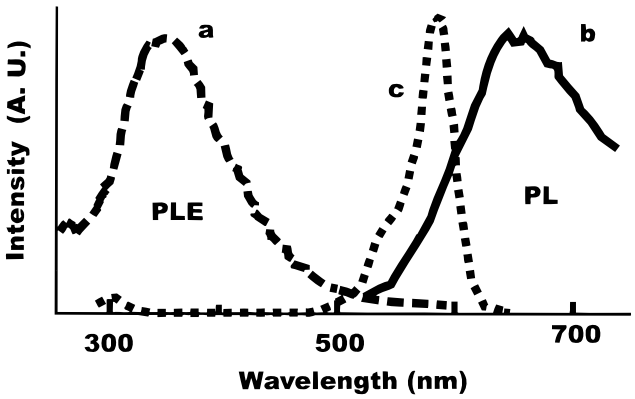

Figure 3. Spectral properties of PS and DODCI. (a) PS−PLE, (b) PS−PL, and (c) DODCI absorption spectrum.

transformation to the final orange-red emitter,[8,22] and (2) the longer wavelength features contributing initially to the orange-red emission are seen to decay most rapidly leading to what appears to be the manifestation of a blue shift of this spectral feature in the absence of etching.

After 5.5 μs, for the aqueous etched sample, and 9.5 μs for the hybrid etched sample, the observed spectral features have merged and change little with delay time as the emission signal, over the gate width of the scan, begins to decrease. These histograms indicate the manner in which the spectral emission intensity depicted in Figure 1 builds to the observed distribution. A comparison with Figure 1 suggests how the dominant characteristics of the 1.5−100 μs spectra develop over the time span of the histograms. With longer time delays, the monitored emission (Figure 2), while maintaining an identical wavelength dependence, decreases precipitously in intensity. The data clearly demonstrate a nearly parallel although clearly different development of the PL intensity for the aqueous and hybrid etches and an overall longer time spectral luminescence which is quite similar for these etched samples.

Dye-Treated Porous Silicon. In our initial dye sensitization experiments, to clearly evaluate the nature of the dye−PS interaction, we have utilized the common dyes DODCI and Rhodamine 700 because of their negligible absorbance in the 350 ± 20 nm range, the approximate peak absorption range of the PS excitation spectrum.[6] Figure 3, parts a−c, demonstrates that DODCI is an optimal choice. While Figure 3a depicts a typical PS ultraviolet excitation spectrum (PLE)[6,14] and Figure 3b demonstrates the resulting orange-red PL from porous silicon, the absorption spectrum for DODCI depicted in Figure 3c demonstrates a very minimal absorbance for $\lambda\lambda$ = 330−470 nm.[36] Rhodamine 700 is also a reasonable candidate, although this dye does display a clear absorbance at λ < 330 nm.[34]

These experiments focus specifically on creating an environment for the energy transfer pumping of the adsorbed dye and/or the mediation of the fluorescence from PS due to PS−dye complexation. As the optical pumping of the PS surface is known to access a long-lived excited-state triplet exciton,[19] we view this excited state as an energy reservoir for subsequent energy (or electron) transfer between the PS surface and the adsorbed dye. Such transfer might take place through fast intermolecular electron transfer pumping of a dye molecule in close proximity to the PS surface. Alternatively, if the dye is chemisorbed to the surface active exciton it could receive the exciton energy via fast intramolecular energy transfer along a short bonding chain. Finally, the presence of this much more efficient radiator could enhance the PS emission rate simply through complexation with the PS fluorophors.

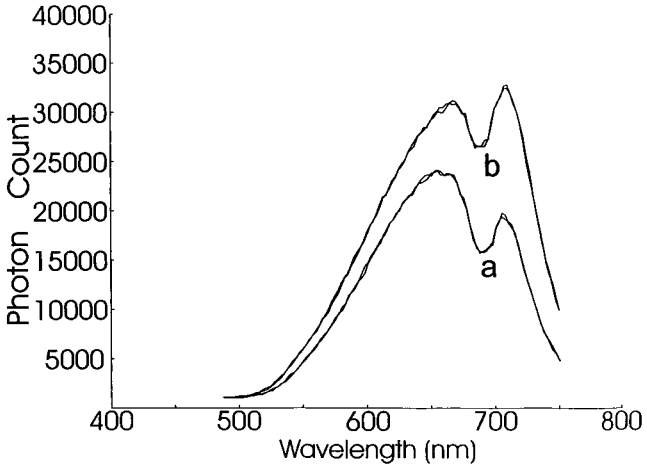

Figure 4. Comparison of time-gated 1.5−100 μs scans of the photoluminescent emission from porous silicon (PS) following excitation of (a) a nanoporous PS sample generated in an aqueous etch, dipped for several seconds in a 10^{-3} M solution of Rhodamine 700 and stored for several months (air) in darkness, and (b) a nanoporous PS sample generated in an aqueous etch, dipped for several seconds in a 10^{-3} M solution of DODCI and stored for several months (air) in darkness. Uncorrected for system response which dips slightly at 690 nm.

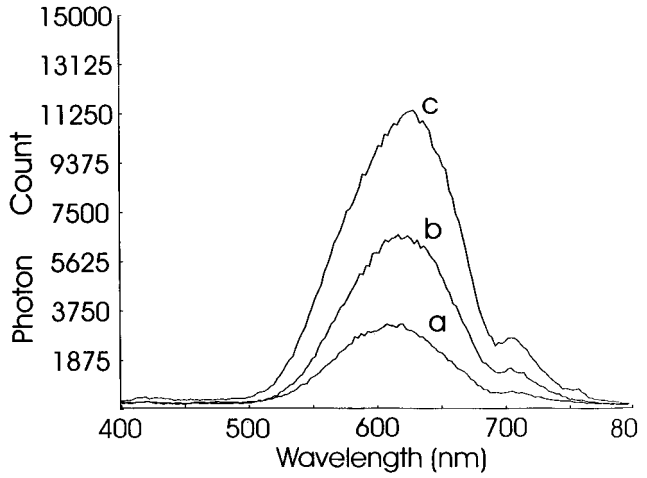

Figure 5. Comparison of time-gated 1.5−100 μs scans of the photoluminescent emission from porous silicon (PS) following excitation of (a) a hybrid (see text) PS sample, placed in a 10^{-3} M solution of Rhodamine 700 for 45 min and stored for several months, (b) a hybrid (see text) PS sample, placed in a 10^{-3} M solution of DODCI for several seconds and stored for several months, and (c) a hybrid (see text) PS sample, placed in a 10^{-3} M solution of DODCI for 45 min and stored for several months. Uncorrected for system response.

Samples exposed to DODCI or Rhodamine 700 dye, when pumped at 337.1 nm, display an initial quenching of the PS photoluminescence followed by an expected slow and continued increase in the PL emission rate upon aging in the dark, in air, for an extended period. The aging cycle eventually produces a PL signal which appears to have maximized and maintained itself for a period of several months. Figure 4 displays the time-dependent photoluminescent emission (uncorrected for system response) from aged aqueous samples which have been dipped for several seconds in 10^{-3} M DODCI and Rhodamine 700. Figure 5 displays the time-dependent PL emission spectra (uncorrected for system response) for hybrid etched samples which have been soaked in 10^{-3} M DODCI and Rhodamine 700 for 45 min, comparing these to the emission from a hybrid etched sample exposed for only a few seconds to DODCI. In Figures 4 and 5 the spectra are taken over the time frame 1.5−100 μs after the nitrogen laser excitation pulse. For all of the

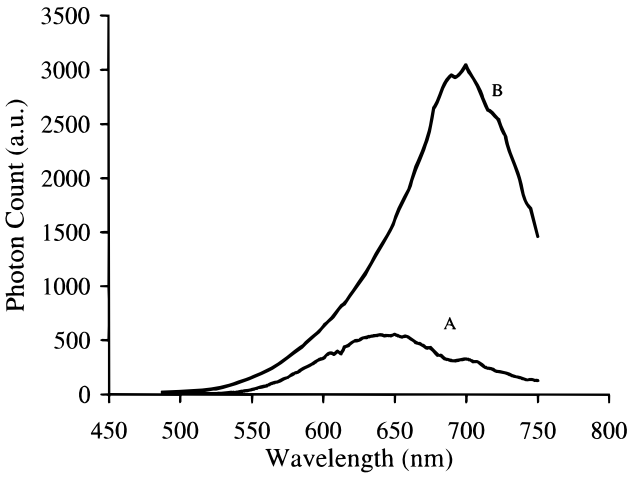

Figure 6. Comparison of the photoluminescence spectrum of (a) a typical aqueous etched PS sample with that of (b) a PS sample laden with DODCI. Luminescent intensities were acquired 15 ns after the illumination pulse. Note the shoulder apparent at ∼700 nm. Corrected for system response.

experiments conducted on DODCI and Rhodamine 700, we have observed little or no clear emission on the time scale of nanoseconds (5−100 ns). Further, under comparable conditions we have established that the nitrogen laser does not excite fluorescence from 10^{-3} M samples of DODCI or Rhodamine 700.

After some period of aging, the DODCI-treated sample in Figure 5a is found to display a photoluminescence (Figure 6), corrected for phototube and system response, which exceeds the intensity of a nominally prepared PS sample by a factor greater than 5. Further, as Figure 6 demonstrates, the distribution of fluorescence is *notably* broader with a peak response considerably red shifted (∼30−50 nm) from an aqueous etched untreated PS sample. This is consistent with one of the PS-dye couplings which we have previously considered. Note that, as opposed to high-temperature annealing at temperatures between 100 °C[31] and a very significant 600 °C[30] for short periods to promote oxidation on the PS surface, we facilitate a long-term aging process under conditions which promote the conversion of the surface and ensure a dye-initiated modification *without seriously modifying the interacting constituencies*.

Photoluminescence histograms reveal considerably more detailed information on the time evolution of the systems. Figures 7−12 display detailed histograms for the dye-treated aqueous and hybrid samples considered in this study and demonstrate a number of distinct features associated with dye interaction. These histograms, in conjunction with the data in Figures 4 and 5, demonstrate that simple immersion or prolonged soaking of the PS structure in millimolar dye solutions is sufficient not only to position the dye in close proximity to the surface-bound PS emission centers but also to promote its interaction with these centers. The most pronounced interaction is manifest for those samples treated in DODCI. The effects observed for both DODCI and Rhodamine 700 are greatest for those samples treated after aqueous etch.

Figure 7 displays an extensive histogram for delays, after laser pumping, ranging from 0.5 to 61.5 μs (5 μs gate) for a DODCI-treated aqueous etched sample. Here we observe an eventual convergence of the spectral scans to a dominant feature peaking at ∼650 nm, the approximate peak wavelength of the DODCI spectrum in Figure 4. In Figure 8, we compare the PL for time delays of 0.5−11.5 μs (5 μs gate) to the evolution observed for an untreated aqueous etched sample. The DODCI-treated sample

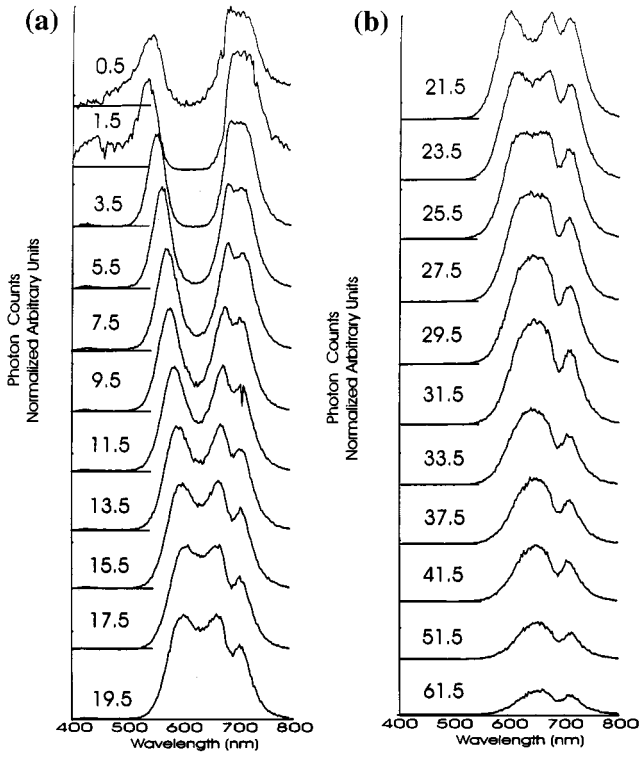

Figure 7. Photoluminescence histogram of a DODCI-treated aqueous etched nanoporous silicon (PS) sample for delay times after nitrogen (337.1 nm) laser pumping of (a) 0.5−19.5 μs, and (b) 21.5−61.5 μs, each with a 5 μs gate. The aqueous etched sample was exposed to a 10^{-3} M solution of DODCI for several seconds and subsequently stored (air) in darkness for several months. Uncorrected for system response.

is clearly distinct, displaying initially both a green emission feature and an "orange-red-red" emission feature which at first appear to "bookend" the observed aqueous etch emission features (Figure 2, 0.5−5.5 μs delay). With increased delay time, Figure 7 demonstrates that the green emission feature red shifts. The red emission feature (uncorrected for system response) appears to split into two features, one of which blue shifts with increased delay time and a second peak which appears to shift to a much lesser extent with time, first to the blue and then to the red, settling to a peak in the vicinity of 710 nm. This gives the appearance of a triple peaked spectrum for time delays ranging from 7.5 to 23.5 μs. After a 27.5 μs delay, the strongly red shifting short wavelength and blue shifting orange-red features have virtually merged into each other as we observe a dominant peak at $\sim$ 640 nm which eventually red shifts by $\sim$10 nm. The observed spectra after 27.5 μs suggest that the continued red shift of the initial green emission feature dominates the characteristics of the observed time dependence. The peak spectral intensity observed in the histograms remains virtually constant out to 33.5 μs and then begins to decrease.

As Figure 9 demonstrates, the interaction of Rhodamine 700 with an aqueous etched PS sample appears to be much less pronounced than that of DODCI. The shifting green and orange-red emission features have merged at the 7.5 μs delay scan to a dominant spectral peak at 640 nm which red shifts to 650 nm by 21.5 μs. Further, the drop-off in spectral intensity occurs considerably more rapidly. Also the $\sim$710 nm (shoulder in system corrected spectrum) feature appears weaker.

The histogram depicted in Figure 10 was obtained for a DODCI-treated hybrid etched sample (Figure 5a) initially soaked for 45 min in a 10^{-3} M dye solution. The dye has a clear effect on the hybrid etched sample although it is not as pronounced

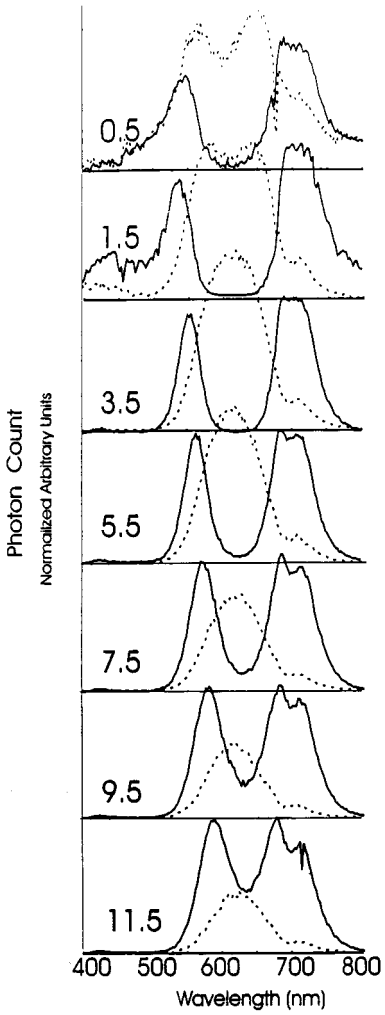

Figure 8. Comparison of photoluminescence histograms for DODCI (10^{-3} M solution) treated (solid line) and untreated (dashed line) aqueous etched porous silicon samples (note also Figures 2a and 7) for delay times after nitrogen (337.1 nm) laser pumping of 0.5−11.5 μs, each with a 5 μs gate. Uncorrected for detection system response.

as that on the aqueous etched sample. Further, a more extended period of exposure to the dye is required as a hybrid sample dipped for several seconds in DODCI is found to display a PL histogram which rapidly converges to a strongly dominant 630−640 nm feature, a behavior indicative of the untreated hybrid etch. In Figure 11, we compare the PL for the DODCI-treated sample to the evolution for an untreated hybrid etched sample for time delays of 0.5 to 9.5 μs (5 μs gate). The histograms of Figures 10 and 11 clearly display the cycle of convergence for the strongly red-shifting green and blue-shifting orange-red emission features. However, the appearance of the triple peaked spectrum ($\tau_{delay} \geq 3.5$ μs) and the time delay corresponding to the merging of the shorter wavelength and orange-red emission features to a dominant 630 nm (peak) feature, $\sim$11.5 μs, occur on a considerably shorter time scale. The spectral intensity of the DODCI-treated sample begins to drop off rapidly for time delays longer than 17.5 μs, converging to a final peak wavelength for the dominant feature at 650 nm.

Figure 12 depicts the histogram for a Rhodamine 700-treated hybrid etched sample. It suggests that even a 45 min exposure has only a small effect. In fact, the convergence of the spectral features to a dominant single peak appears to occur even more rapidly than the untreated sample over the range of delay times of order 3.5 μs or less. A significant drop-off in spectral intensity is observed to occur for time delays longer than 7.5 μs.

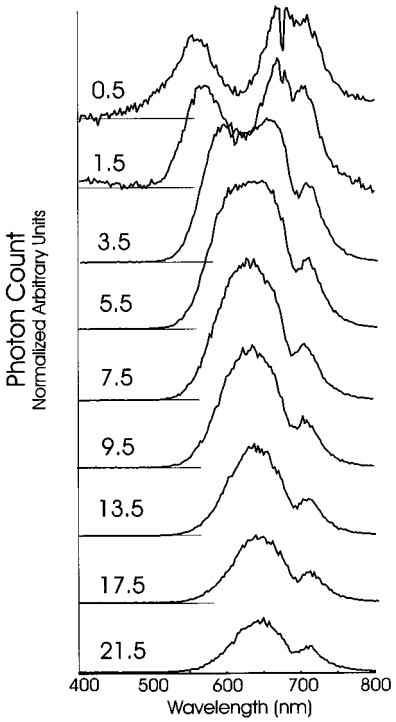

Figure 9. Photoluminescence histogram of a Rhodamine 700-treated aqueous etched nanoporous silicon (PS) sample for delay times after nitrogen (337.1 nm) laser pumping of 0.5 to 21.5 μs, each with a 5 μs gate. The aqueous etched sample was exposed to a 10^{-3} M solution of Rhodamine 700 for several seconds and subsequently stored (air) in darkness for several months. Uncorrected for detection system response.

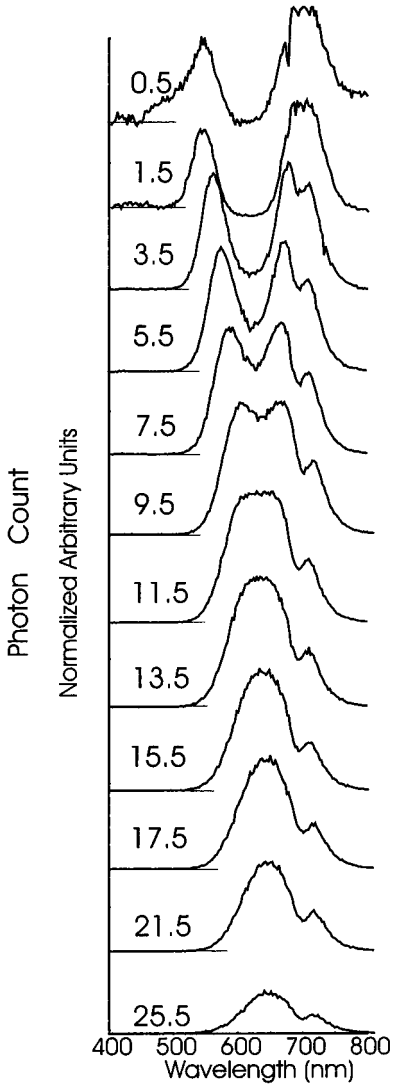

Figure 10. Photoluminescence histogram for a DODCI-treated hybrid macroporous−nanoporous PS (see text) sample for delay times after nitrogen (337.1 nm) laser pumping of 0.5−25.5 μs, each with a gate width of 5 μs. The hybrid sample was exposed to a 10^{-3} M solution of DODCI for 45 min and subsequently stored (air) in darkness for several months. Uncorrected for detection system response.

Discussion

The data presented in Figures 6−12 certainly suggest the coupling of select dyes to the PS surface. The results presented in Figures 7 and 10 demonstrate that a dye sensitization of the PS surface is quite feasible.

The green and orange-red PL emissions characteristic of PS can be excited with a variety of UV light sources and observed during and directly following the in situ (in solution) etching of a PS surface in 20% HF in MeOH or 20% HF in H_2O solutions.[21,22,24] Experimental observations of the time-dependent behavior of this in situ PL[22] can be combined with a quantum chemical modeling[21,24] of the low-lying electronic states of the silanone-based silicon oxyhydrides to suggest that the initially observed and relatively long-lived green PL might best be associated with a precursor silanone state. The subsequent transformation to a final orange-red emitter is then associated with the oxidative conversion of this initially formed silanone-based silicon oxyhydride to create a silanol-like structure.

In Tables 1 and 2, we summarize the results of molecular electronic structure calculations on the silanone-based silicon oxyhydrides. SiO bond lengths and adiabatic energy separations calculated at the MP2/DZP level of description[21−25] for the ground-state singlet and lowest-lying excited-state triplet of the silanone-based oxyhydride compounds[21−25] would appear to be quite consistent with the absorption and emission characteristics which are observed for the UV-excited photoluminescence from a PS surface. The locations of the unsaturated silanone-based silicon oxyhydride triplet states and the known peak wavelength of the porous silicon (PLE) excitation spectrum ($\sim$ 350 nm) bear a close resemblance. The large change in the SiO bond lengths indicated in Table 1, which is not characteristic of the silylene isomers, in turn, produces a large shift in the excited-state potential relative to the ground state.[21−25] This location of the ground- and excited-state potentials can promote optical pumping high up the excited-state potential suggesting that a shift to higher energies, relative to the adiabatic energy separations, should characterize the peak in the PLE excitation spectrum ($\sim$350 nm). This shift should also be accompanied by a significant red shift in the subsequent PL emission range ($\sim$580−800 nm).

When an −OH or $-OSiH_3$ group is bound to a silicon−oxygen double bond in the silanone-based oxyhydrides, the change, Δr (SiO), in transition (Table 1) is consistently of order 0.17 Å (adiabatic energy increment $\sim$3.05 eV).[21,24,25] However, for $Si(O)H_2$, $Si(O)H(SiH_3)$, and $Si(O)(SiH_3)_2$, the change in bond length is notably smaller, decreasing from 0.155 to 0.121 Å, suggesting that the peaks of the PLE and PL spectral profiles associated with these silanones will not be shifted relative to each other to the extent of those silanones containing an −OH or −OR group.[21−25]

Based on the data in Tables 1 and 2, we suggest that the source of the $\sim$520 green emission feature is a precursor state −H or −R group bound (to SiO) silanone-based oxyhydride.[22] If the 520 nm green emission feature is associated with a

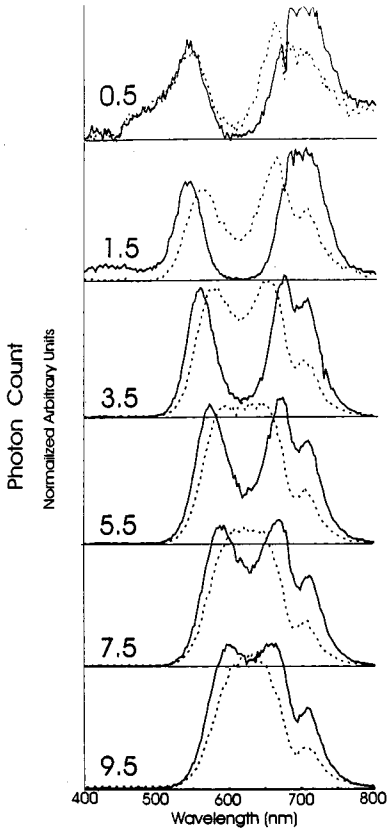

Figure 11. Comparison of photoluminescence histograms for DODCI (10^{-3} M solution) treated (solid line) and untreated (dashed line) hybrid macroporous−nanoporous PS (see text) samples. (Note also Figures 2b and 10) for delay times after nitrogen (337.1 nm) laser pumping of 0.5−9.5 μs, each with a 5 μs gate.Uncorrected for detection system response.

transition involving a long-lived excited triplet state,[22] we suggest that the observed time-dependent (τ_{decay}) tranformation of the 520 nm fluorescence feature in air (Figure 2) can reasonably be attributed to an enhanced excited-state oxidation which converts the initial oxyhydride to the −OH or −OR bound fluorophors subsequently emitting at much longer wavelength.

The data in Figures 7 and 10 clearly demonstrate the continual shift to longer wavelength of the initial 520 nm green emission feature as one samples the emission at longer time delay. We associate this shift, at least in part, with the products of the excited-state oxidation of the long-lived triplet precursor state. This behavior appears analogous to that recently observed in an ENSOM study.[35] The relative intensity of the green emission feature and the rate of its conversion for the DODCI-treated sample (Figure 7) versus the standard aqueous etch (Figure 2) would suggest that a coupling of the dye to the PS surface (1) slows the conversion process and (2) enhances the rate at which the precursor state emits. The data in Figure 7, for the range of time delays from 21.5 to 31.5 μs, suggest that the changing emission from the oxidized precursor state, while first merging with the blue-shifting orange-red emission feature, is the primary influence producing the net red shift of the dominant PL emission feature for $\tau_{delay} > 27.5$ μs.

As the histogram of Figure 7 also demonstrates, an initially dominant red emission feature gives rise to two features, one of which correlates with a significant shift to shorter wavelength with increased time delay while the other, to a much smaller extent, appears to first blue and then red shift in the region around 710 nm. While it might be tempting to assign this red emission feature to a DODCI-dominated dye emission, DODCI, when flashlamp pumped (absorption maximum in ethanol, 582 nm), is known to emit on a much shorter time scale[34] over a narrow region close to 662 nm (peak). Therefore, the observed

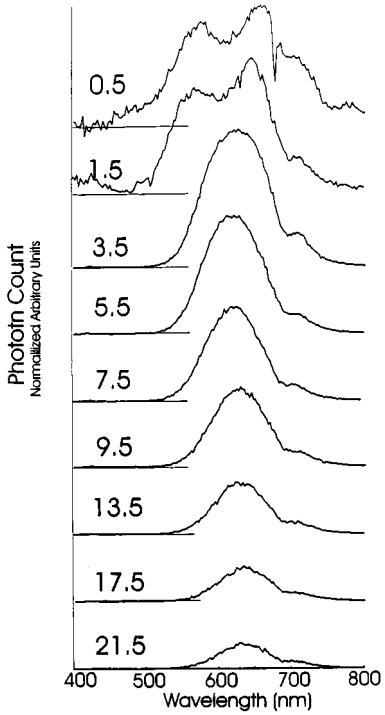

Figure 12. Photoluminescence histogram of a Rhodamine 700-treated hybrid macroporous−nanoporous PS (see text) sample for delay times after nitrogen (337.1 nm) laser pumping of 0.5 to 21.5 μs, each with a gate width of 5 μs. The hybrid sample was exposed to a 10^{-3} M solution of Rhodamine 700 for 45 min and subsequently stored (in air) in darkness for several months. Uncorrected for detection system response.

TABLE 1: Si═O Bond Lengths (Å) for Silanones at the MP2/DZP Level of Description

molecule	*r*(SiO) singlet	*r*(SiO) triplet	Δ*r*(SiO)
$Si(O)H_2$	1.545	1.700[a]	0.155
$Si(O)(SiH_3)_2$	1.560	1.681	0.121
$Si(O)H(SiH_3)$	1.553	1.695	0.142
Si(O)H(OH)[b]	1.537	1.709	0.172
$Si(O)SiH_3(OH)$	1.543	1.712	0.169
$Si(O)H(OSiH_3)$	1.537	1.708	0.171
$Si(O)SiH_3(OSiH_3)$	1.543	1.712	0.169
$Si(O)(OH)_2$	1.536	1.709	0.173
$Si(O)(OSiH_3)_2$	1.537	1.708	0.171

[a] Bond length for the excited singlet is 1.705 Å. [b] Bond lengths for HO−Si−OH silylene are 1.670 Å for the ground-state singlet and 1.680 Å for the excited triplet.

TABLE 2: Ground-State Singlet-Excited-State Energy Separations for Silanones and Silylenes

molecule	Δ*E*(S − T) (kcal/mol)	Δ*E*(S − T) (eV)	$\sim\lambda_{adiabatic}$ (nm)
$Si(O)H_2$	60.1	2.60	475
$Si(O)(SiH_3)_2$	53.9	2.34	530
$Si(O)H(SiH_3)$	57.3	2.48	499
Si(O)H(OH)	70.9	3.07	403
$Si(O)SiH_3(OH)$	71.3	3.09	401
$Si(O)H(OSiH_3)$	70.4	3.05	406
$Si(O)SiH_3(OSiH_3)$	69.6	3.02	411
$Si(O)(OH)_2$	71.1	3.08	402
$Si(O)(OSiH_3)_2$	67.1	2.91	426
HSiOH	38.4	1.66	744
HOSiOH	64.2	2.78	445
SiH_3OSiH_3	67.4	2.92	425

emission in Figure 7 is red shifted to a far greater extent than would be expected for a physisorbed dye on the PS surface. Further, the delay time for emission from a nascent DODCI dye impregnating the PS framework would be expected to be considerably shorter. These considerations and the continual blue shift of the red emission feature with time delay, to a luminescence peaking in the region of the PL for an untreated PS sample, suggest that we are observing the manifestation of emission from a PS−dye complex.

If DODCI complexes with the PS surface structure, we anticipate a distribution of PS−dye complexes. The complexing of a strongly emitting dye to PS is expected to enhance the overall emission rate. Within this framework, we expect a dominance of one or the other participant in the complexation which will be manifest in the emission process by (1) a range of complex radiative lifetimes and (2) a shift in emission features with degree of complexation. We also anticipate that the lifetimes for these dye complexes will decrease with an increased dye coupling. This expectation is, in fact, consistent with the data in Figures 7 and 10, where, with increased time delay, the spectral features appear to be increasingly similar to that of a native PS-dominated emitter.

We also realize that the observed emission intensity for the DODCI-treated samples (Figures 7 and 10) does not drop off nearly as rapidly as that for the untreated aqueous or hybrid etches. In fact, the emission features in the histogram of Figure 7 do not decrease significantly in intensity until we reach a time delay of 33.5 μs. This suggests either a large increase in dye-catalyzed sample formation or a decrease in the emission lifetime for comparable samples that are dominantly PS-emitters but have undergone a strong interaction with the dye. We favor the latter interpretation. The results depicted in Figure 7 suggest that the distribution of emission for PS-based luminescent species has been shifted to a shorter time window. The histograms presented in Figures 2 and 7−11 describe sufficiently different time rates of decay and intensity distributions with time so as to clearly suggest a coupling to the PS surface which is influenced by the bulk structure of the PS substrate. In a sense, we might equate the dye to a strong perturber of the donor−acceptor levels in these doped silicon constituencies.

The feature peaking at 710 nm is also intriguing for its observation even as a shoulder in Figure 6 (corrected for phototube response) may also result from an enhanced emission rate due to dye complexation. We note that the triplet−singlet (ground state) transitions for the corresponding silylene isomers HSiOH (Table 2), $SiH_3SiOSiH_3$ ($Si(O)(SiH_3)_2$), and $HSiOSiH_3$ or SiH_3SiOH ($Si(O)H(SiH_3)$) will all be located close to this spectral region. The interaction of the silylenes, which can be obtained upon the photoisomerization of the silanones, with DODCI would be expected to enhance their respective emission rates promoting the observation of their signature emissions. It is relevant that we associate these transitions with a minimal change in surface fluorphor bonding, signaling a much smaller shift in the spectral distribution with decay time.[21]

The importance of the outlined results is that they demonstrate a definite PS−dye coupling and suggest a distribution of dye−PS interactions for a nanostructured PS matrix. A more definitive assessment of the degree of PS−dye complexation should be obtained from FTIR spectroscopy. However, these experiments will require the generation of a significantly larger PS sample volume which will be the focus of future efforts in our laboratory. We have chosen a long-term aging process to promote the conversion of the PS surface under conditions which ensure the dye-initiated modification of the surface. Once assessed, this long-term process might be used to gauge a much shorter-term annealing oxidation cycle. These experiments, in turn, suggest that an analogous dye sensitization of the PS surface is feasible and that the complementary experiments, which involve either energy-transfer pumping or electron transfer to the PS matrix after dye excitation, are also feasible using such dyes as Rhodamine 6G, Fluorescein, or DCM.

Acknowledgment. We thank Peter Lillihei for his preparation of the hybrid PS samples. We thank Professor Lawrence Bottomley for useful discussions. We acknowledge financial support from the Office of the President at Georgia Institute of Technology under the auspices of the Focused Research Program and the National Science Foundation under Grant PHY-9531372.

References and Notes

(1) Canham, L. T. *Appl. Phys. Lett.* **1990**, *57*, 1046.
(2) (a) Kanemitsu, Y. *Phys. Rep.* **1995**, *263*, 1−92. (b) John, G. C.; Singh, V. A. **1995**, *263*, 93−152.
(3) Prokes, S. M. *J. Mater. Res.* **1996**, *11*, 305.
(4) Collins, R. T.; Fauchet, P. M.; Tishler, M. A. *Phys. Today* **1997**, *50*, 24.
(5) Cullis, A. G.; Canham, L. T.; Calcott, P. D. *J. Appl. Phys.* **1997**, *82*, 909.
(6) See, for example, Brus, L. E.; Szajowski, P. F.; Wilson, W. L.; Harris, T. D.; Schuppler, S.; Citrin, P. H. *J. Am. Chem. Soc.* **1995**, *117*, 2915.
(7) Koch, F.; Petrova-Koch, V.; Muschik, T.; Nikolov, A.; Gavrilenko, V. *Mater. Res. Soc. Symp. Proc.* **1993**, *283*, 197.
(8) (a) Koch, F.; Petrova-Koch, V.; Muschik, T. *J. Lumin.* **1993**, *57*, 271. (b) Koch, F. *Mater. Res. Soc. Symp. Proc.* **1993**, *298*, 222.
(9) See, for example, Calcott, P. D. J.; Nash, K. J.; Canham, L. T.; Kane, M. J.; Brumhead, D. *J. Phys. Condens. Matter.* **1993**, *5*, L91.
(10) Calcott, P. D. J.; Nash, K. J.; Canham, L. T.; Kane, M. J.; Brumhead, D. *J. Lumin.* **1993**, *57*, 257.
(11) Nash, K. J.; Calcott, P. D. J.; Canham, L. T.; Needs, R. J. *Phys. Rev. B* **1995**, *51*, 17698.
(12) Cullis, A. G.; Canham, L. T.; Calcott, P. D. *J. Appl. Phys.* **1997**, *82*, 909.
(13) (a) Schuppler, S.; Friedman, S. L.; Marcus, M. A.; Adler, D. L.; Xie, Y. H.; Ross, F. M.; Chabal, Y. J.; Harris, T. D.; Brus, L. E.; Brown, W. L.; Chaban, E. E.; Szajowski, P. J.; Christman, S. B.; Citrin, P. H. *Phys. Rev. B* **1995**, *52*, 4910. (b) Schuppler, S.; Friedman, S. L.; Marcus, M. A.; Adler, D. L.; Xie, Y. H.; Ross, F. M.; Harris, T. D.; Brown, W. L.; Brus, L. E.; Citrin, P. H. *Phys. Rev. Lett.* **1994**, *72*, 2648.
(14) Xie, Y. H.; Wilson, W. L.; Ross, F. M.; Mucha, J. A.; Fitzgerald, E. A.; Macauley, J. M.; Harris, T. D. *J. Appl. Phys.* **1992**, *71*, 2403.
(15) (a) Prokes, S. Glembocki, O. J.; Bermudez, V. M.; Kaplan, R.; Friedersdorf, L. E.; Pearson, P. C. *Phys. Rev. B* **1992**, *45*, 13788. (b) Prokes, S. M. *J. Appl. Phys.* **1993**, *73*, 407.
(16) (a) Prokes, S. M.; Glembocki, O. J. *Phys. Rev. B* **1994**, *49*, 2238. (b) Prokes, S. M.; Carlos, W. E.; Glembocki, O. J. *Phys. Rev. B* **1994**, *50*, 17093. (c) Carlos, W. E.; Prokes, S. M. *J. Appl. Phys.* **1995**, *78*, 2129. (d) Prokes, S. M.; Carlos, W. E. *J. Appl. Phys.* **1995**, *78*, 2671.
(17) Fuchs, H. D.; Rosenbauer, M.; Brandt, M. S.; Ernst, S.; Finkbeiner, S.; Stutzmann, M.; Syassen, K.; Weber, J.; Queisser, H. J.; Cardona, M. *Mater. Res. Soc. Proc.* **1993**, *283*, 203.
(18) Stutzmann, M.; Brandt, M. S.; Rosenbauer, M.; Fuchs, H. D.; Finkbeiner, S.; Weber, J.; Deak, P. *J. Lumin.* **1993**, *57*, 321.
(19) Brandt, M. S.; Stutzmann, M. S. *Solid State Commun.* **1995**, *93*, 473.
(20) Steckl, A. J.; Xu, J.; Mogul, H. C.; Prokes, S. M. *J. Electrochem. Soc.* **1995**, *142*, L69−71.
(21) Gole, J. L.; Dixon, D. A. *Phys. Rev. B* **1998**, *57*, 12002.
(22) Gole, J. L.; Dixon, D. A. *J. Phys. Chem.* **1998**, *103*, 33.
(23) Gole, J. L.; Dudel, F. P.; Seals, L.; Reiger, M.; Kohl, P.; Bottomley, L. A. *J. Electrochem. Soc.* **1998**, *145*, 3284.
(24) Gole, J. L.; Dudel, F. P.; Grantier, D.; Dixon, D. A. *Phys. Rev. B* **1997**, *56*, 2137.
(25) Gole, J. L.; Dixon, D. A. *J. Phys. Chem.* **1998**, *102B*, 1768.
(26) Dudel, F. P.; Gole, J. L. *J. Appl. Phys.* **1997**, *82*, 802.
(27) Seals, L.; Dudel, F. P.; Grantier, D.; Gole, J. L.; Bottomley, L. *J. Phys. Chem.* **1997**, *101*, 8864.
(28) Warntjes, M.; Veillard, C.; Ozanam, F.; Chazalviel, J. N. *J. Electrochem. Soc.* **1995**, *142*, 4138.

(29) Gole, J. L.; Divincentis, J. A.; Seals, L.; Lillihei, P.; Narasimha, S. Correlation of Porous Silicon Pore Structure with Photovoltaic Response and Photoluminescence−A Connection Between Bulk and Surface Properties, *J. Phys. Chem.*, submitted.

(30) Li, P.; Li, W.; Ma, Y.; Fang, R. *J. Appl. Phys.* **1996**, *80*, 490.

(31) Canham, L. T. *Appl. Phys. Lett.* **1993**, *63*, 337.

(32) Gorbounoua, O.; Mejiritski, A.; Torres-Filho, A. *J. Appl. Phys.* **1995**, *77*, 4643.

(33) Letant, S.; Vial, J. C. *J. Appl. Phys.* **1997**, *82*, 397.

(34) *Lambda Physik Dye Handbook*. (Wall Chart). Also, (a) Rulliere, C. *Chem. Phys. Lett.* **1976**, *43*, 303. (b) Maeda, M.; Miyazoe, Y. *Jap. J. Appl. Phys.* **1972**, *11*, 692. (c) Sibbett, W.; Taylor, J. R. *IEEE J. Quantum Electron.* **1984**, *QE-20*, 108. (d) Antonov, V. S.; Hohla, K. L. *Appl. Phys.* **1983**, *B32*, 9.

(35) Moyer, P. J.; Cloninger, T. L.; Gole, J. L.; Bottomley, L. A. Experimental Evidence for Molecule-Like Absorption and Emission of Porous Silicon Using Near-Field and Far-Field Optical Spectroscopy. *Phys. Rev. B*, submitted. Moyer, P. J.; Gole, J. L. To be published.